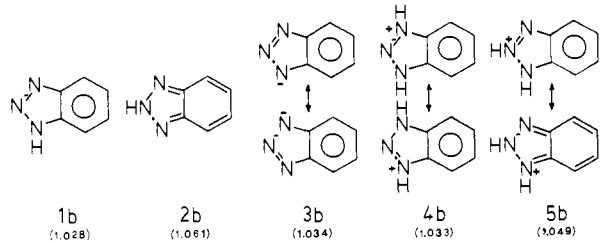

Figure 3. More representative canonical forms of benzotriazoles and ratio $2r_{56}/(r_{45} + r_{67})$.

The aromaticity of both 1,2,3-triazole tautomers being probably similar, the lone pair/lone pair repulsion accounts for the lack of stability of tautomer **1a**. If we assume[2] that the lone pair/lone pair repulsion amounts of 6.5 kcal mol^{-1}, then, in the absence of such an effect, tautomer **1a** would be 1.8 kcal mol^{-1} more stable than **2a**. In the case of benzotriazoles, the aromaticity of the benzenoid tautomer **1b** being obviously greater than that of the quinonoid tautomer **2b**, the situation is reversed. We can estimate the difference in aromaticity between both tautomers as 9.5 kcal mol^{-1}.

In the case of cations, the annellation modifies the difference in energy by 1.4 kcal mol^{-1} only (−13.6 kcal mol^{-1} in favor of **4a**[1] to −15.0 kcal mol^{-1} in favor of **4b**). This small variation is due to the fact that the 1,2-cation is only slightly less aromatic than the 1,3-cation.

Cannonical forms of the five benzotriazole structures together with the $2r_{56}/(r_{45} + r_{67})$ (r being the bond lengths of Table III) are given in Figure 3, where the relationship between stability and localization of the π-system in the benzene ring becomes apparent. (The quinonoid character increasing in the order **1b** < **4b** ≃ **3b** < **5b** < **2b**).

Acknowledgment. We gratefully acknowledge Grant PB0227 from the Spanish C.I.C.Y.T. The skillful assistence of Gunilla Gräntz and Concha Foces-Foces is gratefully acknowledged.

Supplementary Material Available: Tables of experimental geometries of benzotriazoles, 6-31G//6-31G total atomic electronic densities (q_T) and gross orbital populations (q_π) of 1,2,3-triazole derivatives, eigenvalues ϵ_i in au and orbital symmetry, and rotational constants (in megahertz) (4 pages). Ordering information is given on any current masthead page.

(39) Cook, M. J.; Katritzky, A. R.; Linda, P. Aromaticity of Heterocycles. *Adv. Heterocycl. Chem.* **1974**, *17*, 255-356.
(40) Katritzky, A. R.; Barczynski, P.; Musumarra, G.; Pisano, D.; Szafran, M. *J. Am. Chem. Soc.* **1989**, *111*, 7-15.

Comprehensive Theoretical Study of Vinylsilane Primary Dissociation Pathways

J. S. Francisco

Contribution from the Department of Chemistry, Wayne State University, Detroit, Michigan 48202. *Received February 10, 1989*

Abstract: Primary dissociation pathways have been investigated for vinylsilane by ab initio molecular orbital methods. Reactant, transition-state structures, and products were fully optimized at the HF/3-21G and HF/6-31G* levels of theory. Relative energies have been calculated at the MP4SDTQ/6-31G* level of theory, while zero-point energies and vibrational frequencies are calculated at the HF/3-21G level. With these barrier heights and vibrational frequencies, a unimolecular dissociation rate constant $k(E)$ has been determined by using RRKM theory for the primary dissociation channels for vinylsilane. Together these data are used to assess available experimental kinetic data for vinylsilane. The barrier height of the 1,1-H_2 elimination channel is predicted to be 64.4 kcal/mol, while that for the 1,2-SiH_2 elimination channel is predicted to be 68.7 kcal/mol. These theoretical results agree very well with experimental barrier heights for these two lowest channels. However, a *new* primary dissociation pathway is predicted to be competitive with the 1,1-H_2 and 1,2-SiH_2 elimination channels. This finding is discussed in light of previous experimental results on vinylsilane.

The thermal decomposition of vinylsilane has been studied extensively by thermal shock tube studies.[1,2] Despite these thermal studies, the chemistry of the simplest alkenylsilane, CH_2=CH-SiH_3, is not well characterized. Whether the primary dissociation reaction proceeds to generate stable species or reactive intermediates that induce long radical chain reactions is still open to question for these systems. However, vinylsilane holds particular interest not only because it is the simplest alkenylsilane but also because knowledge of its chemistry is essential in assisting experimental identification of reactive intermediates that are implicated in the deposition of amorphous silicon. To data, much of the chemistry of vinylsilane has been speculated on the basis of results from alkylsilanes such as methylsilane[3-6] and ethylsilane.[1,7-12] With vinylsilane there is a large number of primary products that can be produced from unimolecular decomposition as follows:

$$CH_2{=}CHSiH_3 \rightarrow CH_2CHSiH_2 + H \quad (1)$$
$$\rightarrow CH_2CSiH_3 + H \quad (2)$$
$$\rightarrow CHCHSiH_3 + H \quad (3)$$
$$\rightarrow CH_2 + CHSiH_3 \quad (4)$$
$$\rightarrow CHCH_2 + SiH_3 \quad (5)$$
$$\rightarrow C_2H_3SiH + H_2 \quad (6)$$
$$\rightarrow C_2H_4 + SiH_2 \quad (7)$$
$$\rightarrow HCCH_2(SiH_3) \quad (8)$$
$$\rightarrow HCCSiH_3 + H_2 \quad (9)$$
$$\rightarrow CCHSiH_3 + H_2 \quad (10)$$
$$\rightarrow C_2H_2 + SiH_4 \quad (11)$$
$$\rightarrow CH_2CSiH_2 + H_2 \quad (12)$$
$$\rightarrow CH_3SiH_3 \quad (13)$$
$$\rightarrow :C{=}CH_2 + SiH_4 \quad (14)$$

(1) Ring, M. A.; O'Neal, H. E.; Rickborn, S. F.; Sawrey, B. A. *Organometallics* **1983**, *2*, 1891.
(2) Rickborn, S. F.; Ring, M. A.; O'Neal, H. E.; Coffey, D., Jr. *Int. J. Chem. Kinet.* **1984**, *16*, 289.
(3) Davidson, I. M. T.; Ring, M. A. *J. Chem. Soc., Faraday Trans. 1* **1980**, *76*, 1530.

0002-7863/89/1511-7353$01.50/0

Of these channels only a few will dominate the kinetics. Reactions 1–5 are simple homolytic cleavage pathways that involve the breaking of CSi, CH, and SiH bonds. Reactions 6–14 are molecular pathways. Available experimental results[1,2] suggest that reactions 6 and 7 are the lowest energy channels and that reaction 14 is competitive with these two processes. However, more recent theoretical results on ethylsilane[10] suggest that processes similar to reaction 12 are unlikely competitive primary decomposition pathways because they involve high activation barriers (in excess of ca. 100 kcal/mol). In all organosilane systems studied to date it appears that the 1,1-H_2 elimination reaction channel, reaction 6, dominates. However, 1,2-silyl shifts are well-known[13-15] to be low barrier processes. Consequently, we expect that reaction 8 could be competitive with reactions 6 and 7. To assess the relative importance of reactions 1–14, extensive ab initio calculations of the vinylsilane potential surface have been carried out to determine the activation barriers and relative thermodynamic stabilities of each of these channels. With this information and with the aid of RRKM theory calculations we comment on details of the dissociation kinetics of vinylsilane.

Methods

Molecular orbital calculations were performed with the GAUSSIAN 86 system[16] using split valence (3-21G)[17] and polarization (6-31G*)[18] basis sets. All equilibrium geometries and transition-state structures were optimized to better than 0.001 Å for bond distances and 0.1° for bond angles by using analytical gradient methods;[19] with an SCF convergence of at least 10^{-9} on the density matrix, the residual root-mean-square force was always less than 10^{-4} au. Electron correlation energy was estimated by Møller–Plesset perturbation theory[20] up to fourth order, including all single, double, triple, and quadruple excitations (MP4SDTQ, frozen core). Vibrational frequencies and zero-point energies were obtained from analytical second derivatives[21] calculated at the HF/3-21G level by using the HF/3-21G optimized geometry.

Computational Results and Discussion

A. Geometries. The optimized equilibrium geometries for all reactants, products and transition structures are listed in Tables I and II and are shown in Figures 1 and 2. The corresponding total energies are in Table III.

1. Reactants and Products. Calculated structural features for vinylsilane are compared with values derived from microwave

Table I. Optimized Geometries of the Reactants and Products

	$C_2H_3SiH_3$		$C_2H_3SiH_2$		C_2H_3SiH		$HCCH_2(SiH_3)$		$CH_2{=}C{=}SiH_2$		$SiH_3{-}C{\equiv}C{-}H$		CH_2CSiH_3		$CHCH{-}SiH_3$		$:C{=}CH{-}SiH_3$		$H{-}C{-}SiH_3$	
	3-21G	6-31G*	3-21G	6-31G*	3-21G	6-31G*	3-21G	6-31G*	3-21G	6-31G*	3-21G	6-31G*	3-21G	6-31G*	3-21G	6-31G*	3-21G	6-31G*	3-21G	6-31G*
R(SiC)	1.897	1.874	1.871	1.849	1.915	1.881	1.975	1.959	1.703	1.674	1.862	1.838	1.871	1.842	1.906	1.881	1.913	1.890	1.943	1.893
R(CC)	1.322	1.325	1.351	1.352	1.330	1.334	1.463	1.435	1.295	1.301	1.195	1.194	1.328	1.329	1.329	1.330	1.285	1.284		
R(SiH$_1$)	1.488	1.477	1.486	1.476	1.534	1.512	1.479	1.467	1.472	1.463	1.483	1.472	1.491	1.479	1.488	1.476	1.481	1.470	1.483	1.473
R(SiH$_2$)	1.489	1.478	1.487	1.477			1.485	1.474	1.472	1.463	1.483	1.472	1.485	1.474	1.488	1.477	1.483	1.473	1.490	1.480
R(SiH$_3$)	1.489	1.478					1.485	1.472			1.483	1.472	1.485	1.474	1.488	1.477	1.483	1.473	1.492	1.481
R(C$_1$H$_4$)	1.078	1.080	1.078	1.080	1.077	1.080	1.086	1.088			1.052	1.058			1.080	1.082	1.075	1.078	1.096	1.091
R(C$_1$H$_5$)							1.084	1.086												
R(C$_2$H$_4$)									1.078	1.079			1.080	1.082						
R(C$_2$H$_5$)	1.0749	1.077	1.074	1.077	1.076	1.078			1.078	1.079			1.078	1.079	1.070	1.073				
R(C$_2$H$_6$)	1.0752	1.078	1.075	1.077	1.076	1.078	1.099	1.094												
$\angle$SiC$_1$C$_2$	123.8	123.5	124.8	124.6	119.7	118.8	100.1	94.4	180.0	180.0	180.0	180.00	148.3	148.1	123.6	123.1	116.6	114.2		
$\angle$C$_1$SiH$_1$	109.1	109.1	113.6	112.5	96.7	97.3	109.8	109.6	121.2	121.8	109.4	109.5	110.6	110.6	109.0	109.0	109.7	109.4	107.7	109.7
$\angle$C$_1$SiH$_2$	111.0	110.9	113.0	112.1			111.0	112.2	121.2	121.8	109.4	109.5	109.7	109.7	110.8	110.7	108.9	109.1	118.4	118.0
$\angle$C$_1$SiH$_3$	111.0	110.9					105.9	105.1			109.4	109.5	109.7	109.7	110.8	110.7	108.9	109.1	118.4	118.0
$\angle$H$_1$SiH$_2$	109.0	109.0	112.3	111.4			110.4	110.9	117.6	116.5	109.5	109.5	108.9	109.0	109.0	109.2	109.9	110.0	109.1	108.6
$\angle$H$_2$SiH$_3$	107.8	107.6					109.1	108.6			109.5	109.5	108.9	109.0	109.0	109.2	109.6	109.3	108.8	109.0
$\angle$SiC$_1$H$_4$	117.7	117.9	117.1	117.4	122.4	123.6	108.6	109.7	122.0	122.0	180.0	180.0			117.8	118.9	118.0	122.0	115.1	113.7
C$_1$C$_2$H$_4$							108.8	108.3	122.0	122.0			122.5	122.1	118.9	118.0				
C$_1$C$_2$H$_5$	122.4	122.3	121.8	122.0	122.7	122.8			122.0	122.0			121.5	121.9	134.6	134.3				
C$_1$C$_2$H$_6$	122.1	122.2	122.1	122.0	121.7	121.6														
H$_4$C$_1$H$_5$							111.1	111.5												
$\angle$H$_4$C$_2$H$_5$									115.9	116.0			115.9	116.1						
$\angle$H$_4$C$_2$H$_6$	115.5	115.5	116.1	116.0	115.6	115.6														
$\angle$H$_5$C$_2$H$_6$	115.5	115.5	116.1	116.0	115.6	115.6														
$\angle$C(H)CSiH$_1$	0.0	0.0	−151.5	−149.0	180.0	180.0	76.8	83.3	0.0	0.0	0.0	0.0	0.0	0.0	0.0	0.0	0.0	0.0	137.1	147.4
$\angle$SiCCH$_4$							118.4	116.4	0.0	0.0	0.0	0.0			0.0	0.0				
$\angle$SiCCH$_6$	180.0	180.0	3.40	4.2	0.0	0.0	96.7	97.2	0.0	0.0	0.0	0.0								

(4) Sawrey, B. A.; O'Neal, H. E.; Ring, M. A.; Coffey, D., Jr. *Int. J. Chem. Kinet.* **1984**, *16*, 7.
(5) Sawrey, B. A.; O'Neal, H. E.; Ring, M. A.; Coffey, D., Jr. *Int. J. Chem. Kinet.* **1984**, *16*, 23.
(6) Gordon, M. S.; Truong, T. N. *Chem. Phys. Lett.* **1987**, *142*, 110.
(7) Mazel, C. J.; Simons, J. W. *J. Am. Chem. Soc.* **168**, *90*, 2482.
(8) Hase, W. J.; Mazel, C. J.; Simons, J. W. *J. Am. Chem. Soc.* **1973**, *95*, 3454.
(9) Richardson, T. H.; Simons, J. W. *Int. J. Chem. Kinet.* **1968**, *10*, 1055.
(10) Francisco, J. S.; Joyce, S. A.; Steinfeld, J. I.; Walsh, F. *J. Phys. Chem.* **1984**, *88*, 3098.
(11) Rayner, D. M.; Steer, R. P.; Hackett, P. A.; Wilson, C. L.; John, P. *Chem. Phys. Lett.* **1986**, *123*, 449.
(12) Francisco, J. S.; Schlegel, H. B. *J. Chem. Phys.* **1988**, *88*, 3736.
(13) Sakurai, H.; Sakaba, H.; Nakadaira, Y. *J. Am. Chem. Soc.* **1982**, *104*, 6156.
(14) Sakurai, H.; Nakadaira, Y.; Sakaba, H. *Organometallics* **1983**, *2*, 1484.
(15) Nagase, S.; Kudo, T. *J. Chem. Soc., Chem. Commun.* **1984**, 1392.
(16) Frisch, M. J.; Binkley, J. S.; DeFrees, D. J.; Raghavachari, K.; Schlegel, H. B.; Whiteside, R. A.; Fox, D. J.; Martin, R. L.; Fluder, E. M.; Melius, C. F.; Kahn, L. R.; Stewart, J. J. P.; Bobrowicz, F. W.; Pople, J. A. GAUSSIAN 86, Carnegie-Mellon Quantum Chemistry Publishing Unit, Pittsburgh, PA, 1984.
(17) Binkley, J. S.; Pople, J. A.; Hehre, W. J. *J. Am. Chem. Soc.* **1980**, *102*, 939.
(18) Hariharan, P. C.; Pople, J. A. *Theor. Chem. Acta.* **1973**, *28*, 213. Francl, M. M.; Pietro, W. J.; Hehre, W. J.; Binkley, J. S.; Gordon, M. S.; DeFrees, D. J.; Pople, J. A. *J. Chem. Phys.* **1982**, *77*, 3654.
(19) Schlegel, H. B. *J. Comput. Chem.* **1982**, *3*, 214.
(20) Kirshnan, R.; Pople, J. A. *Int. J. Quantum Chem., Quantum Chem. Symp.* **1980**, *14*, 91.
(21) Pople, J. A.; Krishnan, R.; Schlegel, H. B.; Binkley, J. S. *Int. J. Quantum Chem., Quantum Chem. Symp.* **1979**, *13*, 225.

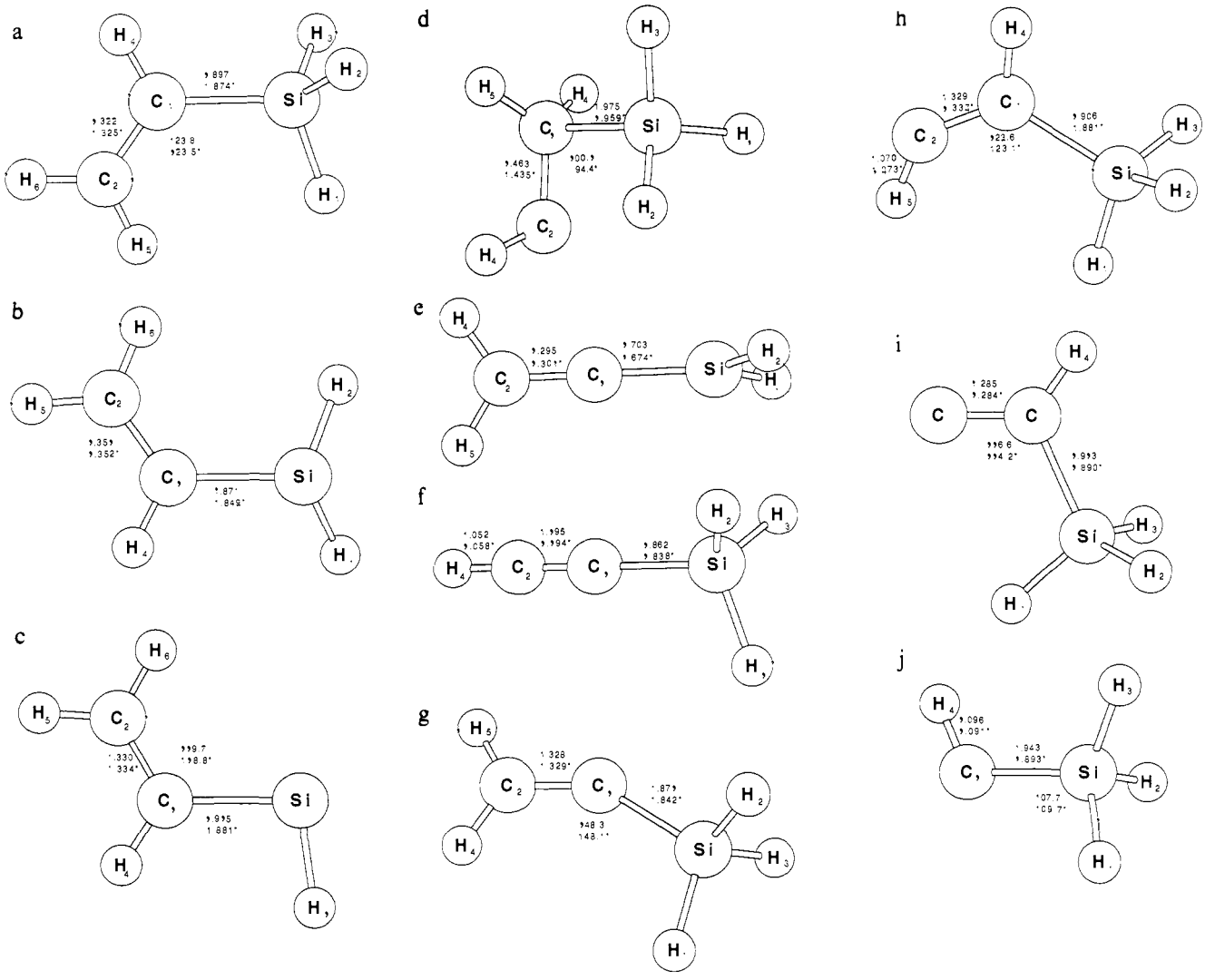

Figure 1. Reactants and products for the dissociation of vinylsilane (HF/3-21G optimized geometry, no superscript; HF/6-31G* optimized, asterisk; see Table I for the complete list of geometrical parameters).

data.[22] The calculated values are shown in Figure 1a. Bond distances and angles at the HF/6-31G* level are in good agreement with the experimental values, and bond angle differences are generally less than ±1°. As an example, our calculated CCSi angle of 123.5° compares well with the experimental value of 122.9 ± 0.3°. We also obtained good agreement with earlier theoretical calculations on vinylsilane.[23-25]

Calculations of equilibrium geometries of the $C_2H_3SiH_2$ radical optimized at the HF/3-21G and HF/6-31G* levels of theory are shown in Figure 1b and in Table I. At the HF/6-31G* level of theory, the CSi bond length is 1.849 Å; this is shorter than that in vinylsilane. Furthermore, it is shorter than the CSi bond lengths in $C_2H_3SiH_2$ (1.899 Å at HF/6-31G*)[12] and CH_3SiH_2 (1.896 Å at HF/6-31G*).[26] Our predictions for the CC bond length and CCSi angle at all levels of theory show these parameters to be larger than those in vinylsilane. These results suggest that there is a tendency for the unpaired electrons to delocalize across the orbitals of the vinyl group in the radical.

The optimized geometry of vinylsilylene (C_2H_3SiH) in its singlet ground state is shown in Figure 1c and Table I. The computed CSi single bond lengths are 1.915 Å (3-21G) and 1.881 Å (6-31G*); these agree with previous calculations on vinylsilylene.[25]

The CSi bond length in silylethylidene ($HCCH_2(SiH_3)$) is 1.959 Å (6-31G*) as shown in Figure 1d, in contrast to vinylsilylene, the corresponding bond ca. 0.06–0.08 Å longer. The CC bond length is predicted to be 1.435 Å at the HF/6-31G* level of theory; this is shorter than the corresponding bond in ethylidene of 1.491 Å at the HF/6-31G* level of theory.[27] The HCC angle in silylethylidene is predicted to be 108.8° (3-21G) and 108.3° (6-31G*), which is slightly greater than that in ethylidene (105.5° at HF/6-31G*).[27] The larger angle in silylethylidene as compared to ethylidene may reflect a greater steric effect due to the silyl group.

The geometry for ethenylidenesilane ($CH_2{=}C{=}SiH_2$) in its singlet ground state is shown in Figure 1e. The CC double bond in this species is shorter than that in vinylsilane by ca. 0.024 Å at the HF/6-31G* level. The CSi double bond agrees well with previous theoretical results (1.703 Å at HF/3-21G);[25] however, our HF/6-31G* calculations suggest that the CSi bond length shortens considerably with the addition of polarization functions to 1.674 Å.

The geometry for 3-sila-1-propyne, found in Table I and Figure 1f, compares well with values derived from the microwave spectrum.[28,29] The CC and CSi bond distances at the HF/6-31G* level are in good agreement with the experimental values (i.e., CC = 1.207 ± 0.006 Å and CSi = 1.826 ± 0.003 Å). The C–H

(22) O'Reilly, J. M.; Pierce, L. *J. Chem. Phys.* **1961**, *34*, 1176.
(23) Oberhammer, H.; Boggs, J. E. *J. Mol. Struct.* **1979**, *57*, 175.
(24) Gordon, M. S. *Chem. Phys. Lett.* **1980**, *76*, 163.
(25) Gordon, M. S.; Koob, R. D. *J. Am. Chem. Soc.* **1981**, *103*, 2939.
(26) Barton, T. J.; Resis, A.; Davidson, I. M. T.; I-Maghsoodi, S.; Hughes, K. J.; Gordon, M. S. *J. Am. Chem. Soc.* **1987**, *108*, 4022.
(27) Raghavachari, K.; Frisch, M. J.; Pople, J. A.; Schleyer, P. v. R. *Chem. Phys. Lett.* **1982**, *85*, 145.
(28) Muenter, J. S.; Laurie, V. W. *J. Chem. Phys.* **1963**, *39*, 1181.
(29) Gerry, M. C. L.; Sugden, T. M. *Trans. Faraday Soc.* **1965**, 2091.

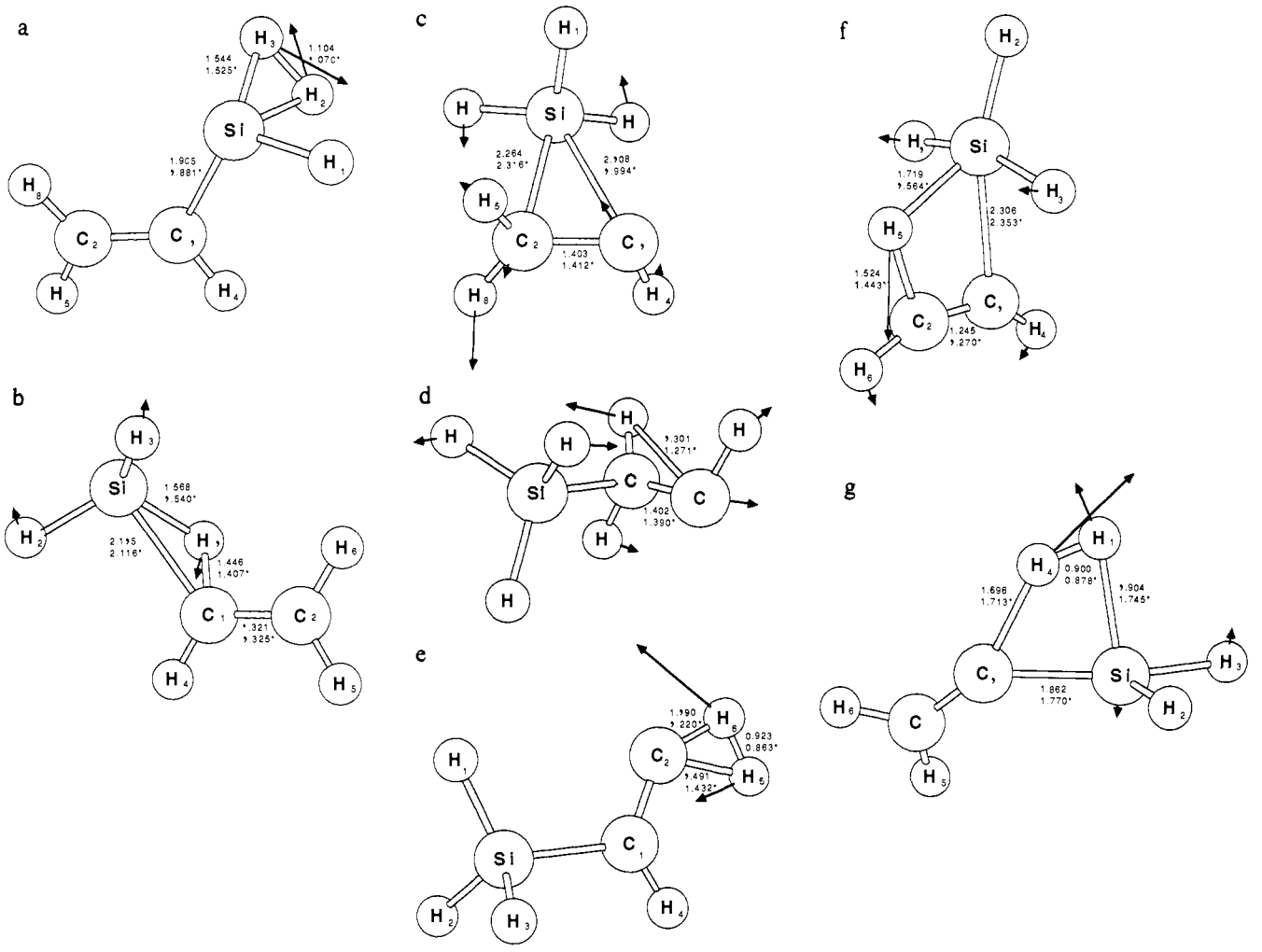

Figure 2. Transition states for the dissociation of vinylsilane (HF/3-21G optimized geometry, no superscript; HF/6-31G* optimized, asterisk; see Table II for the complete list of geometrical parameters).

bond length from microwave measurements is 1.056 ± 0.002 Å and compares very well with the HF/6-31G* value of 1.058 Å.

The geometries of the CH_2CSiH_3 and $CHCHSiH_3$ radicals optimized at the HF/3-21G and HF/6-31G* are shown in Figure 1g,h, respectively, and in Table I. At the HF/6-31G* level of theory, the CSi bond length in $CHCHSiH_3$ is 1.842 Å and compares well with the corresponding bond length in the $C_2H_3SiH_2$ radical. The CC bond length of 1.329 Å (HF/6-31G*) is also greater than that in vinylsilane; this suggests, as in the case of the $C_2H_3SiH_2$ radical the unpaired electron tends to delocalize across the π orbital of the CC bond, thereby reducing the double-bond character. Similar trends are predicted for the $CHCHSiH_3$ radical.

Optimized geometries for silylethenyl radical ($:C{=}CH{-}SiH_3$) are given in Table I and Figure 1i. This radical is an important silicon analogy to vinylidene radical, which has been well characterized experimentally[30] and theoretically.[31-34] The ground state of silylethenyl radical is distinctly bent with an equilibrium bond angle of 123.8 and 123.5° at the HF/3-21G and HF/6-31G* levels of theory, respectively. The CSi bond lengths of 1.913 Å (HF/3-21G) and 1.890 Å (HF/6-31G*) in silylethynyl radical are also close to that in vinylsilylene, which is close to the experimental CSi single-bond length in ethylsilane (ca. 1.866 ± 0.002 Å)[35] and compares well with the theoretical calculated value of 1.893 Å (HF/6-31G*).[12] The CC bond length in silylethenyl radical is predicted to be longer than the corresponding bond length in vinylidene radical. These results suggest a substantial substituent effect in vinylidene radical.

The predicted equilibrium geometry for silylmethylene ($HCSiH_3$) is shown in Figure 1j. Singlet silylmethylene has a CSi bond length of 1.943 Å at the HF/3-21G level; the addition of polarization functions substantially reduces this distance by 0.05 Å. Most theoretical studies to date have used small basis sets,[36,37] and HF/3-21G results are in good agreement with these calculations. Our HF/6-31G* results for the silylmethylene agree quite well with calculations of Goddard et al.[38] using double-ζ + polarization basis sets.

Optimized geometries for the species SiH_2, SiH_4, $:C{=}CH_2$, C_2H_2, and C_2H_4 at the HF/3-21G and HF/6-31G* levels of theory have been previously calculated[12] and are not reproduced here.

2. Transition-State Structures. The 1,1-H_2 elimination reaction is considered to be the predominant decomposition pathway involving alkyl- and alkenylsilane:[1-6,12,39]

$$RSiH_3 \rightarrow RSiH + H_2 \qquad (15)$$

(30) Burnett, S. M.; Stevens, A. E.; Feigerle, C. S.; Lineberger, W. C. *Chem. Phys. Lett.* **1983**, *100*, 124.
(31) Davis, J. H.; Goddard III, W. A.; Harding, L. B. *J. Am. Chem. Soc.* **1978**, *99*, 2920.
(32) Conrad, M. P.; Schaefer III, H. F. *J. Am. Chem. Soc.* **1978**, *100*, 7820.
(33) Osamura, Y.; Schaefer III, H. F. *Chem. Phys. Lett.* **1981**, *79*, 421.
(34) Raghavachari, K.; Frisch, M. J.; Pople, J. A.; Schleyer, P. v. R. *Chem. Phys. Lett.* **1982**, *85*, 145.
(35) Petersen, D. H. Thesis, The University of Notre Dame, South Bend, IN, 1960.
(36) Gordon, M. S. *Chem. Phys. Lett.* **1978**, *54*, 9.
(37) Strausz, O. P.; Gosavi, R. K.; Theodorakopoulous, G.; Csizmadia, I. G. *Chem. Phys. Lett.* **1978**, *58*, 43.
(38) Goddard, J. D.; Yoshioka, Y.; Schaefer III, H. F. *J. Am. Chem. Soc.* **1980**, *102*, 7644.
(39) Baggott, J. E.; Frey, H. M.; Lightfoot, P. D.; Walsh, R. *Chem. Phys. Lett.* **1986**, *125*, 22.

Table II. Optimized Geometries of the Transition Structures

	$C_2H_3SiH + H_2$		$C_2H_4 + SiH_2$		$HCCH_2(SiH)_3$ (1,2-silyl shift)		$HCCH_2(SiH_3)$ (1,2-hydrogen shift)		$SiH_3-CH=C: + H_2$		$C_2H_2 + SiH_4$		$CH_2=C=SiH_2 + H_2$	
	3-21G	6-31G*	3-21G	6-31G*	3-21G	6-31G*	3-21G	6-31G*	3-21G	6-31G*	3-21G	6-31G*	3-21G	6-31G*
$R(SiC_1)$	1.905	1.881	2.155	2.116	2.264	2.361	1.927	1.911	1.904	1.880	2.306	2.353	1.862	1.770
$R(C_1C_2)$	1.322	1.325	1.321	1.325	1.403	1.412	1.403	1.390	1.319	1.325	1.245	1.270	1.320	1.731
$R(SiH_1)$	1.486	1.474	1.568	1.540	1.474	1.465	1.485	1.473	1.483	1.472	1.524	1.505	1.904	1.745
$R(SiH_2)$	1.696	1.651	1.485	1.473	1.480	1.470	1.487	1.475	1.489	1.479	1.479	1.463	1.498	1.489
$R(SiH_3)$	1.544	1.525	1.485	1.473	1.480	1.475	1.487	1.475	1.489	1.489	1.479	1.463	1.483	1.469
$R(C_1H_4)$	1.076	1.078	1.074	1.077	1.094	1.093	1.081	1.086	1.074	1.078	1.059	1.074	1.696	1.731
$R(C_1H_5)$														
$R(C_2H_5)$	1.075	1.073	1.075	1.077	1.081	1.086	1.316	1.272	1.491	1.432	1.524	1.443	1.078	1.083
$R(C_2H_6)$	1.075	1.073	1.075	1.077	1.082	1.087	1.091	1.090	1.190	1.220	1.060	1.068	1.079	1.082
$\angle(SiC_1C_2)$	122.7	122.2	124.4	126.1	77.4	86.0	127.9	128.7	117.0	116.0	83.9	76.2	135.0	140.5
$\angle(C_1SiH_1)$	113.3	112.9	42.1	46.7	104.6	103.4	108.7	109.2	110.2	110.1	157.6	159.8	79.7	86.9
$\angle(C_1SiH_2)$	95.1	94.8	96.5	96.2	88.9	85.2	110.0	109.5	109.9	110.0	80.0	86.1	140.3	137.4
$\angle(C_1SiH_3)$	114.5	113.7	93.8	92.9	131.4	135.2	109.5	108.9	109.9	110.0	80.0	86.1	113.1	114.4
$\angle(H_1SiH_2)$	88.2	85.6	118.2	117.2	109.8	112.2	109.7	109.9	109.6	109.6	99.3	103.1	99.0	97.2
$\angle(H_2SiH_3)$	39.5	39.1	111.2	111.1	106.8	107.9	108.8	108.9	107.7	107.5	160.0	122.9	106.5	107.4
$\angle(SiC_1H_4)$	118.6	118.0	113.6	113.0	109.8	108.4	115.6	115.4	117.4	117.7	131.9	158.9	65.6	60.5
$\angle(SiC_1H_5)$														
$\angle(C_1C_2H_4)$														
$\angle(C_1C_2H_5)$	121.8	121.9	122.0	121.9	117.7	116.8	58.9	59.4	99.5	94.9	109.0	111.8	126.5	125.2
$\angle(C_1C_2H_6)$	122.3	122.3	122.0	121.9	124.9	124.0	110.9	109.2	138.1	126.3	154.2	155.9	119.2	121.0
$\angle(H_4C_1H_5)$														
$\angle(H_4C_2H_6)$														
$\angle(H_5C_2H_6)$	115.9	115.8	116.0	116.2	113.6	112.4	109.3	108.3	38.3	36.9	96.9	92.3	114.4	113.9
$\angle CCSiH_1$	149.4	152.0	84.9	81.7	102.8	100.0	0.4	0.8	0.0	0.0	180.0	180.0	−152.8	−144.7
$\angle SiCCH_4$														
$\angle SiCCH_6$	0.2	0.1	167.7	170.1	123.1	96.4	−11.5	−8.4	180.0	180.0	0.0	0.0	+179.2	178.3

The optimized geometries for the transition state for $C_2H_3SiH + H_2$ (eq 6) are shown in Figure 2a and Table II. The reverse of reaction 6 is the addition of molecular hydrogen to vinylsilylene. Insertion of vinylsilylene into the H_2 bond length shows structural characteristics similar to predictions in silylene insertion into H_2 and in ethylsilylene insertion into H_2. In fact, the r(H–H) bond lengths for vinylsilylene are intermediate between those for silylene and ethylsilylene insertion. Similar trends are predicted to occur in the SiH distances: r(Si–H) = 1.520, 1.638 Å (silylene insertion), 1.525, 1.651 Å (vinylsilylene insertion), 1.531, 1.655 Å (ethylsilylene insertion) at the HF/6-31G* level of theory.

The geometry of the $C_2H_3SiH_3 \rightarrow C_2H_4 + SiH_2$ transition state, presented in Figure 2b and Table II, differs from the transition states for $CH_4 + SiH_2$[6] and $C_2H_6 + SiH_2$;[12] the difference may be due to the fact that the addition of SiH_2 occurs across ethylenic CH bonds. Comparing the CH bond lengths for the $R + SiH_2$ insertion transition states for R = C_2H_4, CH_4, and C_2H_6 (where r(C–H) = 1.446, 1.579, and 1.593 Å, respectively) illustrates this point.

Perhaps the most interesting finding is the transition structure for the 1,2-silyl shift reaction (Figure 2c). The silyl group shifts diagonally across the CC bond to accomplish the interconversion. In the transition state the silyl group is positioned almost under the CC bond, forming a three-membered ring between the CC and Si atoms. As seen from the geometrical parameters, in particular the SiC_1 distance of 2.361 Å (6-31G*), the transition state lies closer to the product ($HCCH_2(SiH_3)$) than to the reactant. The transition state possess one imaginary frequency and is a true first-order saddle point.

The isomerization reaction of vinylsilane can take place via a 1,2-hydrogen shift via reaction 8. The transition-state structure is shown in Figure 2d and in Table II.

The reaction pathway for this reaction has been followed,[40] and we confirm that the reactant, $C_2H_3SiH_3$, connects to $HCCH_2(SiH_3)$ via this transition state.

The next structure is the transition state for the 1,1-H_2 elimination from vinylsilane, i.e.

$$C_2H_3SiH_3 \rightarrow SiH_3CH{=}C: + H_2 \qquad (10)$$

The transition structure for this reaction has C_s symmetry (Figure 2e). We find the H_2 to be constrained to the plane. One would imagine that the minimum-energy path may involve nonplanarity with the H_2 rotating out of plane. For the C_s structure we find one imaginary frequency involving one normal mode of a′ character. The leaving H_2 has a short HH distance of 0.863 Å (6-31G*) in the transition-state structure. This compares favorably to the HH distance for the 1,1-H_2 elimination in ethylene, which is reported to be 0.838 Å (6-31G**).[41] It should be noted that the short HH distance in the transition state indicates a productlike transition state.

Like the 1,2-elimination of SiH_4 in ethylsilane,[12] the same four-center process in vinylsilane involves a tight four-center transition state (Figure 2f). Similarly, the SiH_3 breaks a bond with the carbon and forms a new bond with hydrogen.

The transition structure for the 1,2-elimination of H_2 is shown in Figure 2g. The $CH_2=C=SiH_2$ fragment in the transition structure is quite similar to the product, indicative of a late transition state. At the HF/3-21G level of theory, the breaking of the CH and SiH bonds occurs quite asynchronously, leading to a rather distorted four-center transition state; however, at the HF/6-31G* level the transition structure becomes nearly symmetric as indicated by the CH and SiH bonds of 1.731 and 1.745 Å, respectively. Similar distortions are found for 1,2-hydrogen elimination reactions in C_2H_6,[42] Si_2H_6,[43] CH_3SiH_3,[6] and $C_2H_5SiH_3$.[12]

B. Vibrational Frequencies. The predicted harmonic vibrational frequencies are presented in Table IV. These HF/3-21G frequencies are expected to be ~10–15% overestimated compared to the exact harmonic frequencies, on the basis of a comparison for a range of experimentally characterized vibrations.[44] The vibrational frequencies for the transition structures are all characterized by one imaginary frequency. Those for the 1,1-H_2 elimination reaction 6 closely resemble those of vinylsilane. As in the case of the analogous reaction for ethylsilane,[12] the im-

(40) Gonzales, C.; Schlegel, H. B.; Francisco, J. S. *Mol. Phys.*, in press.

(41) Raghavachari, K.; Frisch, M. J.; Pople, J. A. *Chem. Phys. Lett.* **1982**, *85*, 145.

(42) Gordon, M. S.; Truong, T. N.; Pople, J. A. *Chem. Phys. Lett.* **1986**, *130*, 245.

(43) Gordon, M. S.; Truong, T. N.; Bonderson, E. K. *J. Am. Chem. Soc.* **1986**, *108*, 1421.

(44) Pople, J. A.; Schlegel, H. B.; Krishnan, R.; De Frees, D. J.; Binkley, J. S.; Frisch, M. J.; Whiteside, R. A.; Hout, R. F.; Hehre, W. J. *Int. J. Quantum. Chem.* **1981**, *S15*, 269.

Table III. Total Energies[a]

system	HF/3-21G	HF/6-31G*	MP2/6-31G*	MP3/6-31G*	MP4SDQ/6-31G*	MP4SDTQ/6-31G*
			$C_2H_3SiH_3$			
reactant	−366.153 71	−368.112 51	−368.442 16	−368.474 39	−368.482 41	−368.493 52
			$C_2H_3SiH_3 \rightarrow C_2H_3SiH + H_2$			
transn struct	−366.027 65	−367.980 10	−368.330 60	−368.365 43	−368.373 69	−368.386 26
product	−366.082 94	−368.020 99	−368.356 36	−368.391 30	−368.400 65	−368.412 21
			$C_2H_3SiH_3 \rightarrow C_2H_4 + SiH_2$			
transn struct	−366.022 85	−367.972 17	−368.326 80	−368.357 99	−368.366 39	−368.380 30
product	−366.085 28	−368.031 50	−368.351 41	−368.389 50	−368.399 60	−368.408 73
			$C_2H_3SiH_3 \rightarrow HCCH_2(SiH_3)$ [1,2-silyl shift]			
transn struct	−366.041 54	−368.009 12	−368.330 31	−368.365 54	−368.373 99	−368.384 61
product	−366.046 13	−368.009 31	−368.325 03	−368.361 65	−368.370 31	−368.380 23
			$C_2H_3SiH_3 \rightarrow HCCH_2(SiH_3)$ [1,2-hydrogen shift]			
transn struct	−366.000 44	−367.976 11	−368.305 18	−368.338 58	−368.347 31	−368.358 48
			$C_2H_3SiH_3 \rightarrow SiH_3\text{–}CCH + H_2$			
product	−366.088 17	−368.042 11	−368.381 72	−368.407 57	−368.417 48	−368.430 29
			$C_2H_3SiH_3 \rightarrow SiH_3\text{–}CH{=}C{:} + H_2$			
transn struct	−365.964 42	−367.930 33	−368.271 08	−368.304 08	−368.313 30	−368.325 77
product	−366.025 80	−367.985 42	−368.305 26	−368.341 21	−368.351 64	−368.363 04
			$C_2H_3SiH_3 \rightarrow C_2H_2 + SiH_4$			
transn struct	−365.949 53	−367.932 65	−368.265 60	−368.296 35	−368.306 38	−368.318 87
product	−366.082 94	−368.042 96	−368.371 66	−368.400 47	−368.410 11	−368.422 12
			$C_2H_3SiH_3 \rightarrow CH_2{=}C{=}SiH_2 + H_2$			
transn struct	−365.937 86	−367.903 81	−368.254 44	−368.282 79	−368.291 27	−368.305 45
product	−366.045 29	−367.995 78	−368.344 87	−368.375 60	−368.385 35	−368.399 25
			$C_2H_3SiH_3 \rightarrow SiH_3 + C_2H_3$			
product	−366.013 34	−367.996 41	−368.276 32	−368.314 54	−368.325 31	−368.332 47
			$C_2H_3SiH_3 \rightarrow SiH_3CCH_2 + H$			
product	−366.021 41	−367.981 28	−368.269 61	−368.304 14	−368.313 83	−368.322 31
			$C_2H_3SiH_3 \rightarrow SiH_3CH{=}CH + H$			
product	−366.014 48	−367.972 13	−368.262 21	−368.262 21	−368.305 38	−368.314 19
			$C_2H_3SiH_3 \rightarrow SiH_3CH + CH_2$			
product	−366.853 56	−367.824 14	−368.095 46	−368.144 13	−368.155 69	−368.160 84
			$C_2H_3SiH_3 \rightarrow SiH_2CHCH_2 + H$			
product	−366.047 47	−367.992 19	−368.300 44	−368.332 34	−368.341 43	−368.351 40
			$C_2H_3SiH_3 \rightarrow CH_3CSiH_3$			
product	−366.015 64	−367.981 59	−368.288 89	−368.327 01	−368.335 82	−368.344 46
			$C_2H_3SiH_3 \rightarrow :C{=}CH_2 + SiH_4$			
product	−366.021 48	−367.988 53	−368.292 19	−368.332 43	−368.343 08	−368.352 28

[a] Total energies in au, 1 au = 627.51 kcal/mol.

Table IV. Vibrational Frequencies[a]

	transition structure						
reactant $C_2H_3SiH_3$	$C_2H_3SiH + H_2$	$C_2H_4 + SiH_2$	$HCCH_2(SiH_3)$[b]	$HCCH_2(SiH_3)$[c]	$SiH_3\text{–}CH{=}C{:} + H_2$	$C_2H_2 + SiH_4$	$CH_2{=}C{=}SiH_2 + H_2$
143a″	1724i	1535i	386i	1512i	1626i	1549i a′	1964i
319a′	114	221	271	61	117 a″	247 a′	206
486a″	341	271	479	319	318 a′	387 a′	285
652a′	471	472	538	470	423 a″	535 a″	393
757a′	644	614	634	608	634 a′	599 a′	514
787a″	706	716	764	761	694 a′	674 a″	635
1001a′	762	745	953	770	729 a″	775 a″	659
1017a″	874	975	1010	978	827 a′	823 a′	775
1042a′	1109	991	1043	1016	891 a′	892 a′	885
1153a″	1158	1135	1065	1022	1000 a′	952 a″	1049
1160a′	1171	1156	1170	1214	1015 a″	1069 a″	1129
1183a″	1184	1190	1189	1289	1041 a′	1131 a′	1181
1445a′	1446	1386	1320	1375	1064 a″	1210 a′	1314
1601a′	1538	1562	1385	1429	1341 a′	1291 a″	1563
1807a′	1592	1761	1669	1550	1641 a′	1659 a′	1604
2260a″	1801	1959	2265	2039	1963 a′	1945 a′	1792
2269a′	2113	2277	2318	2281	2260 a″	2056 a′	2090
2278a′	2280	2291	2318	2286	2274 a′	2223 a′	2202
3292a′	3300	3298	3121	2288	2305 a′	2300 a″	2304
3305a′	3323	3353	3222	3143	2702 a′	3500 a′	3251
3369a′	3377	3378	3290	3259	3338 a′	3569 a′	3302

[a] Harmonic vibrational frequencies in cm^{-1} calculated at the HF/3-21G level. [b] [1,2-silyl shift]. [c] [1,2-hydrogen shift].

Table V. Heats of Reaction[a]

level of theory	$SiH_3CCH + H_2$	$C_2H_2 + SiH_4$	$C_2H_3SiH + H_2$	$C_2H_4 + SiH_2$	$SiH_2{=}C{=}CH_2 + H_2$	$HCCH_2{\cdot}(SiH_3)$	$SiH_3{-}CH{=}C: + H_2$	$SiH_3 + C_2H_3$	$SiH_3CCH_2 + H$	$SiH_3CH{=}CH + H$	$SiH_3CH + CH_2$	$SiH_2CHCH_2 + H$	CH_3CSiH_3	$:C{=}CH_2 + SiH_4$
HF3-21G	41.1	44.4	44.4	42.9	68.0	67.5	80.3	88.1	83.0	87.4	188.3	66.7	86.6	109.3
HF6-31G*	44.2	43.6	57.4	50.8	73.2	67.8	79.8	72.9	82.3	88.1	181.0	75.5	82.2	77.9
MP2/6-31G*	37.9	44.2	53.8	56.9	61.1	73.5	85.9	104.1	108.3	112.9	217.6	88.9	92.5	94.1
MP3/6-31G*	41.9	46.4	52.1	53.3	62.0	70.7	83.6	100.3	106.8	112.1	207.2	89.1	92.5	89.1
MP4SDQ/6-31G*	40.7	45.4	51.3	52.0	60.9	70.3	82.1	98.6	105.8	111.1	205.0	88.5	92.0	87.4
MP4SDTQ/6-31G*	39.7	44.8	51.0	53.2	59.2	71.1	81.9	101.1	107.4	112.5	208.8	89.2	93.5	88.6
ΔZPE/3-21G	−8.5	−5.7	−5.2	−2.7	−7.6	−2.2	−10.4	−6.7	−9.9	−9.8	−11.0	−7.1	−2.1	−7.9
$\Delta H°_{rxn}$, 0 K	31.2	39.1	45.8	50.5	51.6	68.9	71.5	94.4	97.5	102.7	197.8	82.1	91.4	80.7

[a] In kcal/mol.

Table VI. Barrier Heights[a]

level of theory	$C_2H_3SiH + H_2$	$HCCH_2(SiH_3)$ [1,2-silyl]	$C_2H_4 + SiH_2$	$HCCH_2(SiH_3)$ [1,2-H]	$SiH_3{-}CH{=}C: + H_2$	$C_2H_2 + SiH_4$	$CH_2{=}C{=}SiH_2 + H_2$
HF3-21G	79.1	70.4	82.1	96.2	118.8	128.1	135.4
HF6-31G*	83.1	64.9	88.1	85.6	114.3	112.9	131.0
MP2/6-31G*	70.0	70.2	72.4	85.9	107.4	110.8	117.8
MP3/6-31G*	68.4	70.2	73.0	85.2	106.9	111.7	120.2
MP4SDQ/6-31G*	68.2	68.0	72.8	84.8	106.1	110.5	119.9
MP4SDTQ/6-31G*	67.3	68.3	71.0	84.8	105.3	109.6	118.0
ΔZPE/3-21G	−2.9	−1.8	−2.3	−4.5	−6.8	−5.0	−6.0
best estimate	64.4	66.5	68.7	80.2	95.8	104.6	112.0

[a] In kcal/mol.

aginary frequency is quite large ($1724i$ cm^{-1})—that for ethylsilane is $1710i$—and is consistent with a narrow barrier. The imaginary frequency for the three-center elimination of SiH_2 corresponds to a 1,2-hydrogen shift mixed with SiH_2 rotation and is similar to SiH_2 elimination in ethylsilane[12] as evidenced by the similarity in magnitude of imaginary frequencies: $1535i$ cm^{-1} for vinylsilane and $1539i$ cm^{-1} for ethylsilane. In the transition structure for 1,2-silyl shift, the imaginary frequency is quite low, $386i$ cm^{-1}; the nature of the transition vector suggests that this motion consists mainly of the CCSi bending mode mixed with the SiH_3 umbrella motion. The vibrational frequencies for the remaining frequencies, for the most part, lie between the frequencies of the reactants and products.

C. Heats of Reaction and Barrier Heights. Table V lists calculated heats of reaction for dissociation pathways of vinylsilane. Unfortunately, there are no experimental measurements for the heats of formation for vinylsilane. Nevertheless, Rickborn et al.[2] have estimated $\Delta H_f°(C_2H_3SiH_3)$ as 21.5 kcal/mol. With this estimate combined with experimental values for heats of formation for SiH_4 ($\Delta H_f° = 8.1 \pm 0.5$ kcal/mol),[45] SiH_3 ($\Delta H_f° = 46.6 \pm 1.4$ kcal/mol),[46,47] SiH_2 ($\Delta H_f° = 65.4 \pm 1.6$),[48,49] C_2H_4 ($\Delta H_f° = 12.54 \pm 0.07$ kcal/mol),[50] C_2H_3 ($\Delta H_f° = 69 \pm 2$ kcal/mol),[51] and C_2H_2 ($\Delta H_f° = 54.55 \pm 0.17$ kcal/mol), we can estimate the reliability of our calculated heats of reactions for dissociation pathways for vinylsilane.

The $\Delta H°$ for $C_2H_3SiH_3 \rightarrow C_2H_2 + SiH_4$ is estimated to be 40.9 ± 0.4 kcal/mol from the above values as compared to 39.1 kcal/mol calculated at the MP4SDTQ/6-31G* level. Similar agreement is obtained between experimental estimated and theoretical heats of reactions for $C_2H_3SiH_3 \rightarrow C_2H_4 + SiH_2$ and $C_2H_3SiH_3 \rightarrow C_2H_3 + SiH_3$. A general trend appears to be that in the highest level of calculation the heats of reaction are overestimated by ca. 5 kcal/mol. Nevertheless, the good agreement suggests that the experimental estimated heat of formation used for vinylsilane is quite reasonable. Thermodynamically, five decomposition pathways appear competitive: elimination of ethynylsilane, 1,2-elimination of SiH_4, 1,1-elimination of H_2 from the silicon end, 1,2-hydrogen shift to yield SiH_2 and C_2H_4, and 1,2-hydrogen elimination to produce ethenylidene silane. The predicted heats of reaction for these five reactions are 31.2, 39.1, 45.8, 50.5, and 51.6 kcal/mol, respectively. The reactions that form substituted carbene and vinylidene species, i.e., $HCCH_2{\cdot}(SiH_3)$ and $SiH_3CH{=}C:$, are higher than the five competitive pathways by ca. 38–40 kcal/mol relative to the lowest thermodynamic channel. One might expect that bond fission processes could compete with the molecular processes; however, most of these processes are thermodynamically unfavorable. The CSi homolytic cleavage process is predicted to be 94.4 kcal/mol. This is considerably higher than most carbon silicon compounds; the average $D°$(C–Si) is estimated as 84 kcal/mol as derived from the bond dissociation energy in $Me_3Si{-}CH_3$[53] and related compounds.[54] The stronger C–Si bond results from the π system of the carbons that interact with orbitals on the silicon to stabilize it.

The energetic ordering of the five thermodynamically competitive pathways changes considerably when the kinetics of these reactions is considered. The activation energy for the elimination of ethynylsilane is nearly 16 kcal/mol greater than that for 1,1-H_2

(45) Gunn, S. R.; Green, L. H. *J. Phys. Chem.* **1961**, *65*, 779.
(46) Doncaster, A. M.; Walsh, R. *Int. J. Chem. Kinet.* **1981**, *13*, 503.
(47) Berkowitz, J.; Greene, J. P.; Cho, H.; Ruscic, B. *J. Chem. Phys.* **1987**, *86*, 1235.
(48) Francisco, J. S.; Barnes, R.; Thoman, Jr., J. W. *J. Chem. Phys.* **1988**, *88*, 2334.
(49) Van Zoeren, C.; Thoman, Jr., J. W.; Steinfeld, J. I.; Rainbird, M. *J. Phys. Chem.* **1988**, *92*, 9.
(50) Rossini, F. D.; Knowlton, J. W. *J. Res. Natl. Bur. Std.* **1937**, *19*, 249.
(51) Benson, S. W. *Thermochemical Kinetics*, 2nd ed.; Wiley: New York, 1976.
(52) Pedley, J. B.; Naylon, R. D.; Kirby, S. P. *Thermochemical Data of Organic Compounds*, 2nd ed., Chapman & Hall: London, 1986.
(53) Baldwin, A. C.; Davidson, I. M. T.; Reed, M. D. *J. Chem. Soc., Faraday Trans. 1* **1978**, *74*, 2171.
(54) Walsh, R. *Acc. Chem. Res.* **1981**, *14*, 246.

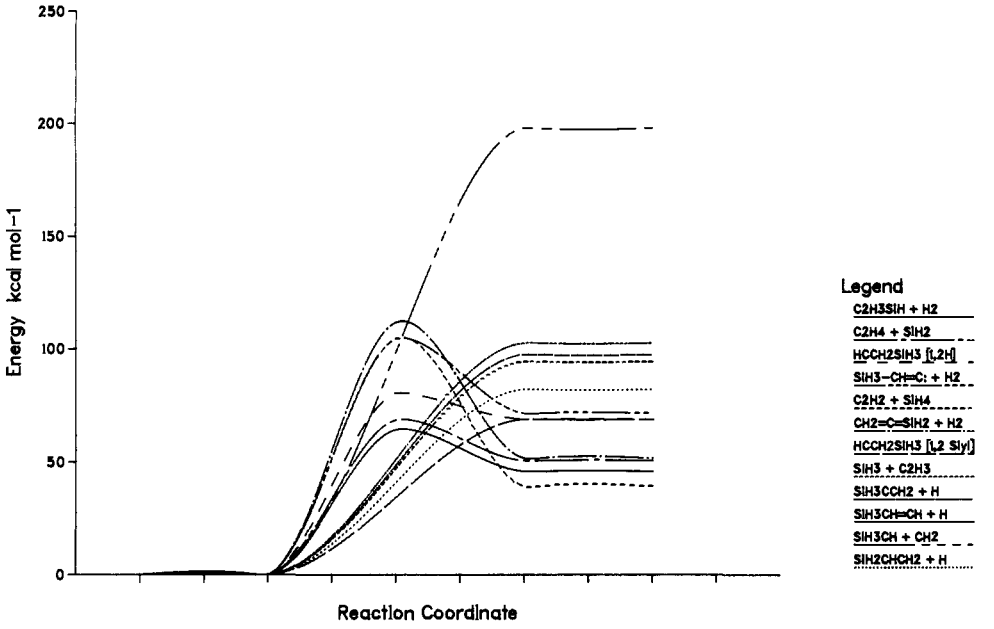

Figure 3. Summary of potential energy surfaces for CH_2=$CHSiH_3$ dissociation.

Table VII. Comparison of Experimental and Theoretical Barrier Heights

system	method	barrier height[a]	ref
$C_2H_3SiH + H_2$	theory	64.4	this work
	experiment	63.3	1
		63.96	2
$C_2H_4 + SiH_2$	theory	68.7	this work
	experiment	63.3	1
		65.9	2

[a] In kcal/mol.

elimination of H_2 to form C_2H_3SiH (as shown in Table VI), even though the former process is thermodynamically more favorable by 14.6 kcal/mol. In fact our calculated activation energy for the 1,1-H_2 elimination to form vinylsilylene is in good agreement with the experimental activation energy from shock tube studies as shown in Table VII. Our estimate of the activation energy is well within 2 kcal/mol of the experimentally measured value. The calculated barrier for 1,2-elimination of SiH_2 to yield ethylene is predicted to be higher than 1,1-H_2 elimination process by ca. 4 kcal/mol. Results from shock tube experiments are consistent with the calculated energetic ordering of these processes, as shown in Table VII.

However, the most interesting finding is the 1,2-silyl shift in reaction 8. Although thermodynamically this reaction is not competitive with the aforementioned processes, kinetically it becomes so. The barrier for this process at the lowest level of theory (HF/3-21G) is calculated as 70.4 kcal/mol. This is nearly 10 kcal/mol lower than the 1,1-H_2 elimination process to form $C_2H_3SiH + H_2$. With a larger basis set the relative energy differences in the activation energy between these processes increase to 18.2 kcal/mol. However, when correlation is added, the 1,1-H_2 elimination process becomes the lowest channel. The estimated activation energy barrier for the 1,2-silyl shift reaction at the MP4SDTQ/6-31G* level falls below the enthalpy for the products of this reaction by 2.4 kcal/mol. This suggests that the reaction has no barrier for the reverse reaction, (-8). Geometries of the reactant and the intermediate have been optimized at the MP2/3-21G* level. From calculation of several points along the path connecting the reactant with the intermediate, no maximum was found, only a smoothly increasing energy profile. Therefore, an estimate of the activation energy for this process is 68.9 kcal/mol. Consequently, a new reaction channel competitive with the two lowest observed reaction pathways is predicted.

(55) Schaefer III, H. F. *Acc. Chem. Res.* **1979**, *12*, 288.

There is another reaction pathway that leads to the same products of reaction 8: a 1,2-hydrogen shift. Such a process is known to take place for ethylene to yield methylcarbene:[27,55]

$$C_2H_4 \rightarrow CH_3CH: \qquad (16)$$

The calculated barrier is 80.7 kcal/mol at the MP4SDQ/6-31G**//HF/6-31G* level of theory.[27] This is in good agreement with the present calculation for 1,2-hydrogen shift yielding $HCCH_2(SiH_3)$ of 80.2 kcal/mol at the MP4SDTQ/6-31G* level with zero-point energy corrections. This process has a barrier of 11.3 kcal/mol for rearrangement back to vinylsilane, i.e., the reverse of reaction 8. It could be the case that rearrangement would not occur via the hydrogen shift but via silyl shift since the latter process has a zero barrier. Furthermore, with $HCCH_2(SiH_3)$ one can obtain scrambling of nuclei, if a deuterium substitution experiment is done, since one can have internal rotation about the CC bond. Consequently, simple deuterium studies could not be used to sort out mechanistic details of vinylsilane decomposition.

For the 1,2-SiH_4 elimination reaction 11, the activation energy exceeds that for the 1,1-H_2 elimination to form vinylsilylene by more than 40 kcal/mol. Consequently, this reaction is not a primary source of SiH_4 in vinylsilane decomposition. It is interesting to note that the predicted activation energy of 105.5 kcal/mol at the MP4SDQ/6-31G* with zero-point energy correction is considerably higher for the 1,2-SiH_4 elimination for ethylsilane at the same level of theory (90.0 kcal/mol). This may result as a consequence of the four-centered transition state for vinylsilane being tighter than that for ethylsilane. The least favorable pathway is the concerted elimination of molecular hydrogen to yield SiH_2=C=CH_2. The activation energy for the process is large (112.0 kcal/mol at the MP4SDTQ/6-31G* level). In the analogous ethylsilane and ethane reactions, the activation energies for the 1,2-elimination of H_2 is also quite high: Si-H_2=$CHCH_3$ (107.1 kcal/mol)[12] and CH_2=CH_2 + H_2 (122.2 kcal/mol).[42] Our estimate of the activation energy for the reaction of CH_2=C=SiH_2 + H_2 appears to be intermediate between these systems. We note that such high barriers in 1,2-H_2 eliminations have been predicted in other organosilicon systems.[6,43]

The 1,2-hydrogen shift reaction leading CH_3CSiH_3 is found not to be an energetically feasible pathway:

$$CH_2{=}CHSiH_3 \rightarrow CH_3CSiH_3 \qquad (13)$$

The potential energy surfaces are summarized in Figure 3.

D. Dynamics of the Unimolecular Dissociation Pathways: RRKM Theory Calculations. To interpret the decomposition

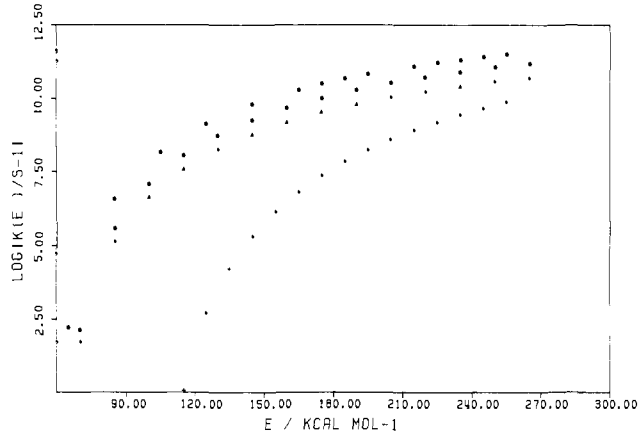

Figure 4. Unimolecular dissociation rates for vinylsilane molecular dissociation pathways as a function of energy: (□) $C_2H_3SiH + H_2$, (●) $C_2H_4 + SiH_2$, (△) $HCCH_2(SiH_3)$, and (+) $CH_2{=}C{=}SiH_2$.

kinetics and assess the relative importance of reaction pathways, we need to know their energy-dependent unimolecular dissociation rates. The simplest approach to obtaining this information is from RRKM theory,[56,57] in which the microcanonical unimolecular rate constant, $k_{RRKM}(E)$ of an isolated molecule with somme total internal energy E is determined. This approach requires only knowledge of the usual transition-state information (i.e., frequencies and internal moments of inertia, for reactant and transition state, and the critical energy for reaction). RRKM calculations are carried out by using the Bunker and Hase RRKM programs.[58] On the basis of earlier results for ethylsilane,[12] we expect that these rate constants should be reliable to ~20–30% for a given set of transition-state parameters.

The results of the RRKM calculations are shown in Figure 4. The salient point of these calculations is that the 1,1-H_2 elimination pathway 6 is seen to be a fast process at relatively low energies and should dominate. At low energies, the 1,2-SiH_2 elimination 7 and 1,2-silyl shift 8 compete with the 1,1-H_2 elimination pathway. For example, at E = 85 kcal/mol, the branching ratio for reactions 7 and 6 is 0.099 and for reactions 8 and 6 is 0.037. This suggests that reaction 7 will comprise ~10% of the overall primary decomposition process and that reaction 8 will make up ~4% of the overall primary decomposition process for vinylsilane. Secondary reaction pathways for $HCCH_2(SiH_3)$ reactions are

$$HCCH_2(SiH_3) \rightarrow SiH_4 + C_2H_2 \quad (17)$$

$$\rightarrow HC{\equiv}CSiH_3 + H_2 \quad (18)$$

The possibility of reaction 17 or 18 occurring is unlikely since no SiH_4 and silylacetylene are reported as an observed reaction product. It may be the case that the $HCCH_2(SiH_3)$ species isomerizes to vinylsilane, which subsequently dissociate via reaction 6. Results from thermal shock tube studies are generally in accord with these predictions. Assuming no secondary reaction source for H_2 formation, the primary process yields for H_2 are about 72–82% of the total dissociation, while the yields for C_2H_4 range from 20–14%. According to the yields reported for $CH_2{=}C{=}SiH_2$ in the shock tube experiments, the 1,2-H_2 elimination of vinylsilane to form $CH_2{=}C{=}SiH_2$ should be the next competitive reaction process. However, according to the present calculation, the branching ratio for reaction 12 is zero at energies ≤ 112

$$C_2H_3SiH_3 \rightarrow CH_2{=}C{=}SiH_2 + H_2 \quad (12)$$

kcal/mol, but a branching ratio reported from the shock tube studies is 0.18. At internal energies up to 300 kcal/mol, the branching ratio never exceeds 2% of the decomposition. Consequently, this suggests that there is another channel for $CH_2{=}C{=}SiH_2$ production probably as a consequence of secondary reaction, i.e., 1,2-hydrogen shift from vinylsilylene, viz.

$$CH_2{=}CH{-}SiH \rightarrow CH_2{=}C{=}SiH_2 \quad (19)$$

A similar process for the 1,2-hydrogen shift in methylsilylene to silaethylene has been studied extensively:[59-61]

$$CH_3SiH \rightarrow CH_2{=}SiH_2 \quad (20)$$

A third most likely competitive reaction pathway is the 1,2-silyl shift reaction 8. It should comprise 4–15% of the primary dissociation yields according to these calculations. Further experimental studies would help clarify the role reaction 8 plays in the decomposition process of vinylsilane.

In shock tube decomposition studies of vinylsilane it was suggested that there are two possible mechanisms to describe observed yields of C_2H_4. The first mechanism involved reactions 6, 7, and 12 with yields of $\phi_6 + \phi_7 = 0.53$ and $\phi_{12} = 0.47$. The second mechanism involved the same reactions but with yields $\phi_6 = 0.68$, $\phi_7 = 0.14$, and $\phi_{12} = 0.18$. Both mechanisms provide reasonable interpretations of the vinylsilane shock tube decomposition data, but both are unable to provide an unambiguous distinction between the relative importance of individual primary and secondary processes. However, the present work does provide some unique insight regarding the mechanism. Reaction 12 is unlikely to occur since the activation energy is 112 kcal/mol. Moreover, yields of ethenylidenesilane must result from secondary dissociation of vinylsilylene. This suggests that the mechanism describing the vinylsilane shock tube data is best represented by one that involves both primary and secondary processes to yield C_2H_4. These calculations suggest that significant yields of C_2H_4 are produced from secondary dissociation and a small contribution results from primary dissociation, viz.

$$CH_2{=}CHSiH_3 \rightarrow C_2H_3SiH + H_2 \quad (6)$$

$$CH_2{=}CHSiH \rightarrow C_2H_4 + Si \quad (21)$$

$$CH_2{=}CHSiH_3 \rightarrow C_2H_4 + SiH_2 \quad (7)$$

Acknowledgment. I thank Wayne State University Computer Center and Chemistry Department for ample provision of computing resources which has made this work possible. I acknowledge the many helpful discussions with H. B. Schlegel. I acknowledge the National Science Foundation for a Presidential Young Investigator Award.

Registry No. $CH_2{=}CHSiH_3$, 7291-09-0.

(56) Marcus, R. A. *J. Chem. Phys.* **1952**, *20*, 359.
(57) Robinson, P. J.; Holbrook, K. A. *Unimolecular Reactions*; Wiley-Interscience: New York, 1972.
(58) Hase, W. L.; Baker, D. L. Program 234, Quantum Chemistry, Program Exchange, Indiana University, Bloomington, 1973.
(59) Gordon, M. S. *Chem. Phys. Lett.* **1978**, *54*, 9.
(60) Yoshioka, Y.; Goddard, J. D.; Schaefer III, H. F. *J. Am. Chem. Soc.* **1981**, 2542.
(61) Grev, R. S.; Scuseria, G. E.; Scheiner, A. C.; Schaefer III, H. F.; Gordon, M. S. *J. Am. Chem. Soc.* **1988**, *110*, 7337.